

Femoral Component External Rotation Affects Knee Biomechanics: A Computational Model of Posterior-stabilized TKA

Mohammad Kia PhD, Timothy M. Wright PhD, Michael B. Cross MD, David J. Mayman MD, Andrew D. Pearle MD, Peter K. Sculco MD, Geoffrey H. Westrich MD, Carl W. Imhauser PhD

Abstract

Background The correct amount of external rotation of the femoral component during TKA is controversial because the resulting changes in biomechanical knee function associated with varying degrees of femoral component rotation are not well

understood. We addressed this question using a computational model, which allowed us to isolate the biomechanical impact of geometric factors including bony shapes, location of ligament insertions, and implant size across three different knees after posterior-stabilized (PS) TKA.

Questions/purposes Using a computational model of the tibiofemoral joint, we asked: (1) Does external rotation unload the medial collateral ligament (MCL) and what is the effect on lateral collateral ligament tension? (2) How does external rotation alter tibiofemoral contact loads and kinematics? (3) Does 3° external rotation relative to the posterior condylar axis align the component to the surgical trans-epicondylar axis (sTEA) and what anatomic factors of the femoral condyle explain variations in maximum MCL tension among knees?

Methods We incorporated a PS TKA into a previously developed computational knee model applied to three neutrally aligned, nonarthritic, male cadaveric knees. The computational knee model was previously shown to corroborate coupled motions and ligament loading patterns of the native knee through a range of flexion.

Implant geometries were virtually installed using hip-to-ankle CT scans through measured resection and anterior referencing surgical techniques. Collateral ligament properties were standardized across each knee model by defining stiffness and slack lengths based on the healthy population. The femoral component was externally rotated from 0° to 9° relative to the posterior condylar axis in 3° increments. At each increment, the knee was flexed under 500 N compression from 0° to 90° simulating an intraoperative examination. The computational model predicted collateral ligament forces, compartmental contact forces, and tibiofemoral internal/external and varus-valgus rotation through the flexion range.

Results The computational model predicted that femoral component external rotation relative to the posterior condylar axis unloads the MCL and the medial compartment; however, these effects were inconsistent from knee to knee. When the femoral component was externally rotated by 9° rather than 0° in knees one, two, and three, the maximum force carried by the MCL decreased a respective 55, 88, and 297 N; the medial contact forces decreased

Funding provided by the Clark and Kirby Foundations (TMW).

Clinical Orthopaedics and Related Research® neither advocates nor endorses the use of any treatment, drug, or device. Readers are encouraged to always seek additional information, including FDA-approval status, of any drug or device prior to clinical use. Each author certifies that his institution approved or waived approval for the human protocol for this investigation and that all investigations were conducted in conformity with ethical principles of research.

Hospital for Special Surgery, New York, NY, USA

T. M. Wright Department of Biomechanics Hospital for Special Surgery 535 East 70th Street New York, NY 10021, USA email: wrightt@hss.edu

All ICMJE Conflict of Interest Forms for authors and *Clinical Orthopaedics and Related Research*® editors and board members are on file with the publication and can be viewed on request.

2017 Knee Society Proceedings

at most a respective 90, 190, and 570 N; external tibial rotation in early flexion increased by a respective 4.6°, 1.1°, and 3.3°; and varus angulation of the tibia relative to the femur in late flexion increased by 8.4°, 8.0°, and 7.9°, respectively. With 3° of femoral component external rotation relative to the posterior condylar axis, the femoral component was still externally rotated by up to 2.7° relative to the sTEA in these three neutrally aligned knees. Variations in MCL force from knee to knee with 3° of femoral component external rotation were related to the ratio of the distances from the femoral insertion of the MCL to the posterior and distal cuts of the implant; the closer this ratio was to 1, the more uniform were the MCL tensions from 0° to 90° flexion.

Conclusions A larger ratio of distances from the femoral insertion of the MCL to the posterior and distal cuts may cause clinically relevant increases in both MCL tension and compartmental contact forces.

Clinical Relevance To obtain more consistent ligament tensions through flexion, it may be important to locate the posterior and distal aspects of the femoral component with respect to the proximal insertion of the MCL such that a ratio of 1 is achieved.

Introduction

Femoral component alignment is an important consideration during TKA because of its influence on patient dissatisfaction, anterior knee pain [2], and long-term implant survival [15, 35]. Excessive internal rotation of the femoral component in relation to the femoral posterior condylar axis can lead to knee pain and

stiffness [22]. Internal rotation also qualitatively increases medial collateral ligament (MCL) tension and gapping between the femur and tibia on the lateral side [1]. To avoid these complications, surgeons often externally rotate the femoral component in an attempt to better balance ligament and contact forces on the medial and lateral compartments and restore patellofemoral and tibiofemoral kinematics [3, 30]. However, the effect of femoral component rotation on the biomechanical function of the knee, namely collateral ligament tension, medial and lateral compartment contact forces, and the resulting kinematics, is not well understood.

A previous biomechanical cadaveric study identified the role of external rotation of the femoral component on knee kinematics [21], but the intra-articular and soft tissue forces were not measured. Computational models have been used to identify the interactions among ligament tensions, contact forces, and kinematics, but have done so in models of a single knee, eliminating the variability that likely occurs with anatomic differences among knees in bony anatomy and ligament insertion sites [7, 9].

The other variation that affects external rotation of the femoral component stems from the bony landmarks by which the rotation is measured. Some surgeons align the posterior cut of the femoral component parallel to the surgical transepicondylar axis (sTEA), which is defined as the line connecting the prominence of the lateral epicondyle to the sulcus of the medial epicondyle [4, 22, 25, 33]. In contrast, others rotate the femoral component a fixed amount relative to the posterior condylar axis [29] attributable in part to the ease in locating this reference axis during surgery. A wealth of data exists describing the relationship

between the transepicondylar axis and the posterior condylar axis [31-33]. For example, Thienpont et al. [32] found that there is a 41% chance of misaligning these two axes if surgeons use a fixed angle of 4° between the posterior condylar axis and the sTEA, indicating that there are large variations in femoral geometry across a population. However, no data exist describing the impact of rotation of the femoral component relative to these clinically relevant aspects of the femoral anatomy on knee kinematics, compartmental contact forces, and ligament tensions through a ROM.

To address these shortcomings and thus provide a more comprehensive description of the effects of external femoral component rotation on ligament and contact forces, and on knee kinematics, we used a previously developed computational model of the tibiofemoral joint [14] to answer the following research questions: (1) Does external rotation unload the MCL and what is the effect on lateral collateral ligament tension? (2) How does external rotation alter tibiofemoral contact loads and kinematics? (3) Does 3° external rotation relative to the posterior condylar axis align the component to the sTEA and what anatomic factors of the femoral condyle explain variations in maximum MCL tension among knees?

Materials and Methods

A computational model of the tibiofemoral joint was used to answer our research questions. The advantage of using a computational knee model was that it enabled us to control for ligament properties, including stiffness and slack length, and frontal plane alignment. With these variables

controlled in the model, we could then isolate the influence of geometric variations across the three knee models on tibiofemoral biomechanics. We have previously shown that this computational knee model predicted mechanics of the intact tibiofemoral joint that agreed with cadaveric measurements including anterior translation and internal rotation (≤ 0.4 mm and 1.6° root mean square [RMS] error, respectively) and collateral ligament forces (≤ 5.7 N RMS error) from full extension to 130° flexion [14].

Three steps were required in building the computational models. First, under institutional review board approval, bony geometries of three neutrally aligned, nonarthritic, male cadaveric legs (ages 20, 21, and 42 years) from the femoral head to the foot were obtained. Each leg was placed in a CT scanner (Biograph mCT; Siemens, Erlangen, Germany), positioned in full extension, and scanned axially with a slice thickness of 0.625 mm and in-plane pixel dimensions of 0.6 mm x 0.6 mm. Subsequently, the CT images were imported into image processing software (Mimics; Materialise, Inc, Leuven, Belgium) to obtain three-dimensional solid geometries of the proximal and distal aspects of the tibia and femur.

For the second step in building the models, femoral and tibial components of a contemporary posterior-stabilized (PS) implant were positioned in the three knees to simulate a TKA. Three-dimensional geometries of the femoral and tibial components of the Optetrak Logic[®] knee (Exactech, Inc, Gainesville, FL, USA) were obtained from computer-aided design files. The femoral component had a thickness of 8 mm both distally and posteriorly. The tibial insert was 9 mm thick. The components were aligned with the femur and tibia using reverse engineering software (Geomagic, Morrisville, NC, USA). The

measured resection technique was followed to position the implant components into the bony geometries [16]. For implanting the tibial component, the proximal tibial cut was aligned perpendicular to the mechanical axis of the tibia (that is, the axis connecting the center of the knee to the center of the ankle obtained from the CT scan) in the coronal and sagittal planes. A maximum of 9 mm of tibial bone was resected using the highest point of proximal tibial bone as a reference and assuming 2 mm of cartilage thickness. Internal rotation of the tibial component was adjusted by aligning the center of the tibial component with respect to the medial one-third of the tibial tubercle [19]. To implant the femoral component, we identified the angle between the femoral mechanical axis (that is, the axis connecting the center of the femoral head to the center of the knee) and the intramedullary axis (anatomic axis) in each knee and then rotated the femoral component in the coronal plane relative to the intramedullary axis by this amount. Thus, the femoral component was aligned perpendicular to the mechanical axis of the femur in the frontal plane. A maximum of 8 mm of bone was resected from the most distal femoral condyle to restore the thickness of the distal femoral component. Next, anterior referencing was used to determine femoral component sizing because it is commonly used with this implant system. The posterior femoral cut was referenced to the posterior condylar axis and rotated externally about the distal diaphysis of the femur by 3° as is standard in clinical practice for typical varus and neutrally aligned knees [29]. The resulting amount of bone removed from the posterior condyles of the three femurs ranged from 3 mm to 12 mm (Fig. 1).

In the third step of building the computational models, collateral and

capsular ligaments were added to link the femoral and tibiofibular geometries. Ligament insertions were defined in detail in our previously published paper [14]. Specifically, insertions were visualized directly by dissecting each of the cadaver knees from which the models were developed and using previous anatomic studies [8, 13, 14, 17, 18, 28]. CT scans of each knee were also inspected to identify bony landmarks corresponding to the ligament insertions. The insertion of the MCL and posterior oblique ligament follow those described by LaPrade et al. [17] and corroborated those identified by Saigo et al. [27]. The ligaments and capsule were represented with a total of 20 tension-only, nonlinear force elements (Fig. 2) with mechanical properties taken from the literature [26, 37]. The MCL was represented with six fibers, divided into distal and proximal groups, each with anterior, central, and posterior fibers [14]. The MCL was modeled to wrap around the medial aspect of the knee. The lateral collateral ligament (LCL) consisted of a single fiber between its femoral and fibular insertions. The slack lengths of the collaterals and capsular ligaments were determined using a previously described optimization algorithm [14] to achieve experimentally measured in situ ligament forces of the intact knee at full extension. The in situ forces of the native MCL and LCL at full extension were used as targets for defining the slack length in the computational models with TKA because this was considered to reflect a balanced knee at full extension. It also provided a common target to standardize the definition of ligament slack length across each knee model to control for this source of knee-to-knee variability in model predictions. Contact force (y) between the articular surfaces of the implant was

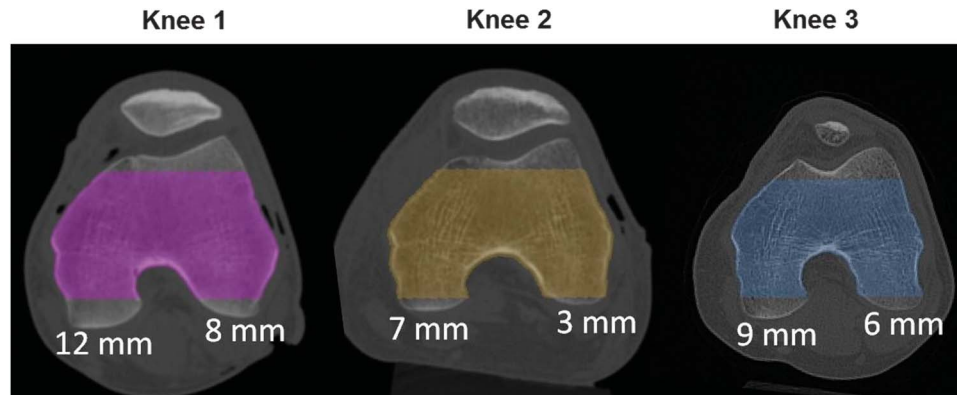


Fig. 1 The amount of bone resected from the posterior femoral condyles varied among the three knees that were modeled for the study. These images show the amount of posterior bone resected with the cuts oriented in 3° external rotation relative to the posterior condylar axis.

defined as a nonlinear function of penetration depth (x), $y = Ax^b$, based on a uniaxial compression test of a metal femoral component on a polyethylene tibial insert. The fit to the experimental data yielded the coefficients: $A = 3986$ and $b = 1.77$ with $R^2 = 0.995$. All details of the models were integrated into the dynamics software (MSC software; Adams,

Newport Beach, CA, USA) to solve the differential equations of motion [14].

To answer our first two research questions, the TKA models were flexed from 0° to 90° because this represents a common range through which surgeons assess the knee intraoperatively. Axial compression of 500 N was applied through flexion to approximate the contact forces measured

intraoperatively using intraarticular force sensors [20]. The femoral component was rotated externally relative to the posterior condylar axis by 0°, 3°, 6°, and 9° to include rotations beyond those typically used by surgeons. The femoral component was rotated about the distal femoral diaphysis to simulate the intraoperative technique for the Optetrak Logic implant. Outputs of the

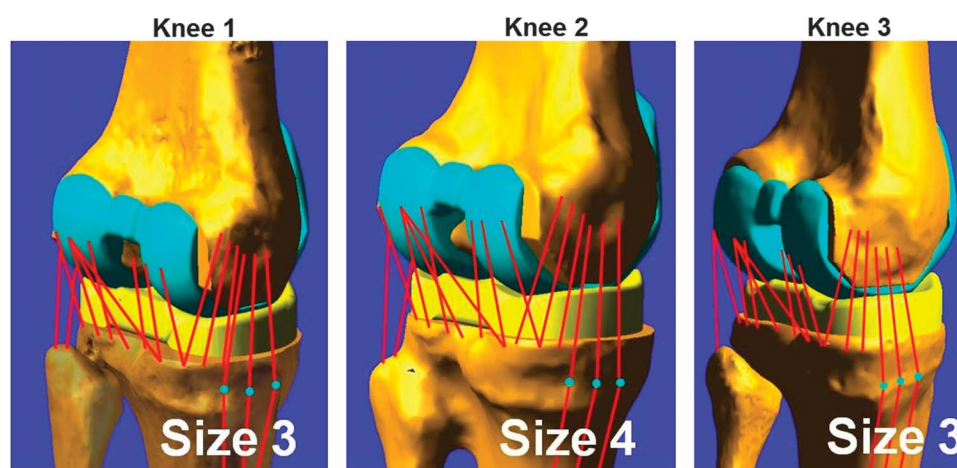


Fig. 2 The three knee models with the TKA components implanted included bony geometries, femoral and tibial component geometries, and ligament fibers. Implant sizes are listed at the bottom right of each image. These images show the femoral component rotated 3° externally relative to the posterior condylar axis.

computational models were the forces carried by the MCL and LCL, the contact forces on the medial and lateral compartments of the tibial component, and tibiofemoral kinematics including internal-external rotation and varus-valgus alignment of the tibia relative to the femur. The results of each knee model were presented individually.

To address our third research question, we identified the rotational alignment of the femoral component relative to the sTEA by overlaying the resected femoral bone geometries on the CT images of the cadaveric knees using the Mimics software. This was done at femoral component rotation of 3°, which is typical for a neutrally aligned or varus knee [29]. The sTEA was identified in the axial plane as the line connecting the most prominent point of the lateral epicondyle and the medial epicondylar sulcus [4, 22, 25, 33]. We then measured the angle between the sTEA and the posterior femoral condylar cut. Finally, we calculated a ratio in each knee between the distances of the medial epicondylar sulcus (the

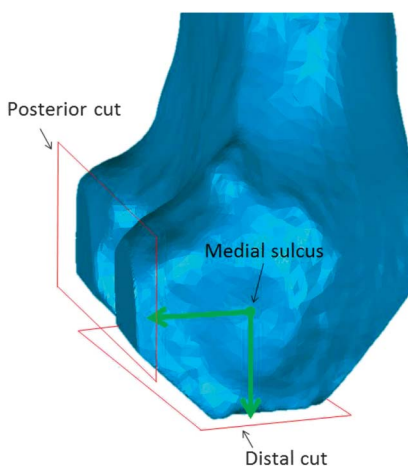


Fig. 3 Distal and posterior distances of the medial epicondylar sulcus (green arrows) to the distal and posterior condylar cuts. This image shows the posterior cut in 3° external rotation relative to the posterior condylar axis.

medial point that defines the sTEA) to the distal and posterior condylar cuts (Fig. 3). We then compared this ratio with the maximum force carried by the MCL in flexion. We also examined femoral component placement with respect to additional features of the femoral anatomy including the proximal insertions of the MCL to identify additional geometric factors related to the maximum force carried by the MCL.

Results

External Rotation and Collateral Ligament Loading

External rotation of the femoral component unloaded the MCL, particularly from 30° to 90° flexion (Fig. 4A-C). The amount of unloading increased with flexion; at 90° of flexion, the maximum force carried by the MCL decreased a respective 55, 88, and 297 N in knees one, two, and three when the femoral component was placed in 9° of external rotation rather than 0°. The anterior MCL fiber carried most of the load, bearing 90%, 90%, and 45% of the total MCL force in knees one, two, and three, respectively, at 90° flexion. LCL tension increased either with higher external rotation of 6° and 9° (knees one and two) or not at all (knee three) (Fig. 4D-F). In knee one, LCL force was a maximum of 40 N when the femoral component was in 9° of external rotation (Fig. 4D). External rotation of the femoral component more strongly influenced knee two; the maximum LCL force was 48 and 138 N with external rotation of 6° and 9°, respectively (Fig. 4E).

External Rotation and Tibiofemoral Contact Loads and Kinematics

Medial compartment contact loads decreased as the external rotation of the

femoral component increased from 0° to 9° (Fig. 5A-C). Increasing femoral component external rotation from 0° to 9° led to a maximum decrease in medial contact forces of 90, 190, and 570 N in knees one, two, and three, respectively. In contrast, the lateral contact force increased by a maximum of 35, 200, and 220 N in knees one, two, and three, respectively (Fig. 5D-F) with external rotation from 0° to 9°. Furthermore, with 3° of external rotation of the femoral component, the contact force was 46, 105, and 392 N greater in the medial compartment than the lateral compartment in knees one, two, and three, respectively, at 90° flexion.

As for the predicted tibiofemoral kinematics in response to the femoral component having been externally rotated at implantation, the tibia rotated externally in full knee extension and rotated externally between full extension and 20° flexion. For example, increasing external rotation of the femoral component from 0° to 9° increased external tibial rotation from 0° to 20° flexion by 4.6°, 1.1°, and 3.3° in knees one, two, and three, respectively. The direction of tibial axial rotation changed abruptly from internal to external rotation between 70° and 80° of flexion with 9° of femoral component external rotation (Fig. 6A-C). In the frontal plane, increasing external rotation of the femoral component from 0° to 9° increased varus by a maximum of 8.4°, 8.0°, and 7.9° in knees one, two, and three, respectively (Fig. 6D-F).

Relationship Between Geometric Features and MCL Loads

External rotation of 3° caused the femoral component to be aligned nearly parallel to the sTEA ($0.7^\circ \pm 0.4^\circ$) in only one knee (Fig. 7). In the other two knees, it was externally rotated relative to the sTEA (by 2.7° and

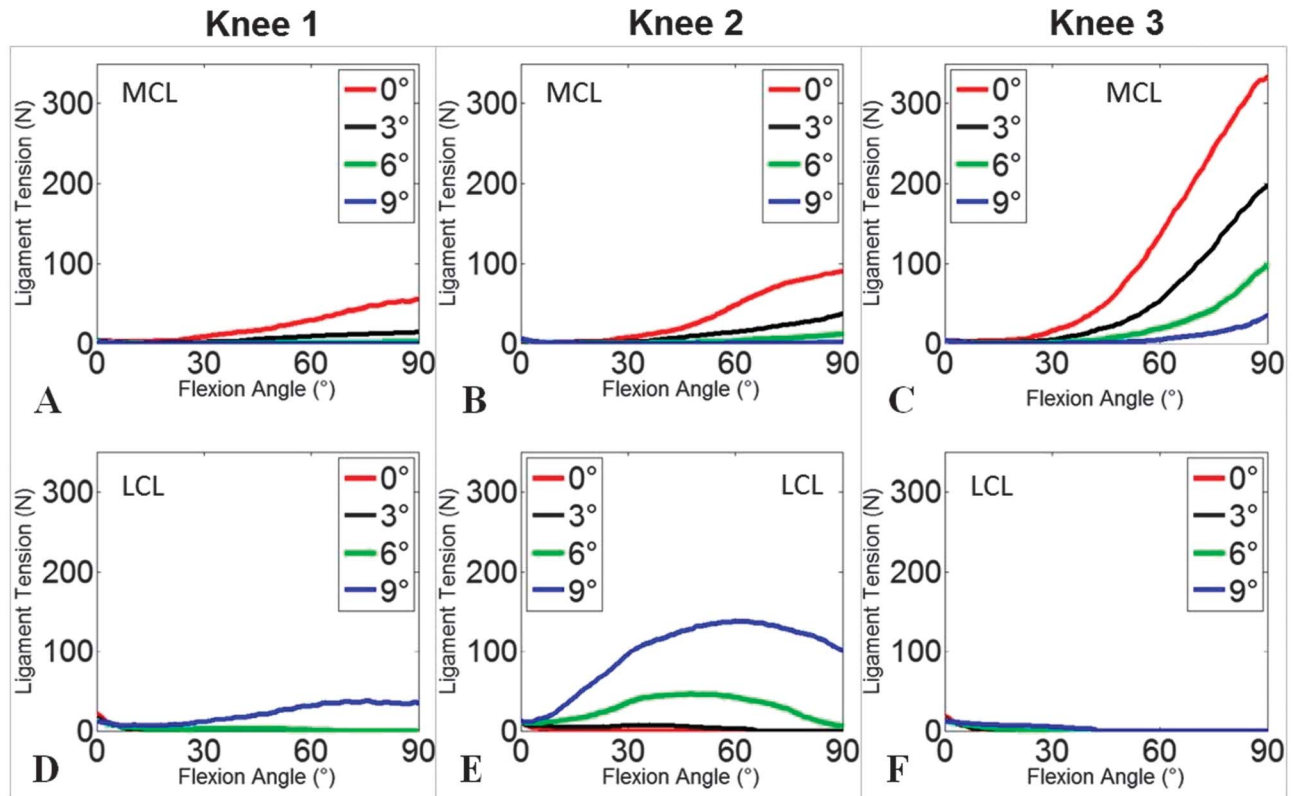


Fig. 4 A-F Collateral ligament tensions predicted by the three knee models were affected through a flexion path from 0° to 90° when the femoral component had been rotated externally at implantation by 0°, 3°, 6°, and 9° relative to the posterior condylar axis: (A-C) MCL; (D-F) LCL.

1.7°; Fig. 7). Moreover, with 3° external rotation of the femoral component, the ratios of the distances of the medial epicondylar sulcus (that is, the most medial point that defines the sTEA) relative to the posterior and distal condylar cuts were 0.86, 0.96, and 1.11 in knees one, two, and three, respectively. The larger the ratio in each knee, the larger the load carried by the MCL at 90° flexion (Fig. 8A-B). Unexpectedly, we found that the maximum force carried by the MCL across the three knees was also related to the ratio of the distances of the proximal insertion of the anterior fiber of the MCL to the posterior and distal condylar cuts. This ratio was 1.18, 1.26, and 1.70 in knees one, two, and

three, respectively; the larger the ratio in each knee, the larger the maximum force carried by the MCL.

Discussion

Selecting the amount of axial rotation of the femoral component during TKA is controversial because the resultant biomechanical effects of this important surgical parameter on collateral ligament forces, compartmental contact forces, and knee kinematics are not well understood. To identify these interactions, we utilized a computational knee model [14] with three unique sets of tibiofemoral geometries. The

computational model allowed us to isolate the biomechanical impact of geometric variations including bony shapes, location of ligament insertions, and implant size after PS TKA across three different knees.

Our study has limitations. The CT data were from three male cadaveric legs. However, the surgical technique in performing TKA is not sex-specific; moreover, the amount of bone resected in our three knee models spanned the range of what is typically removed across both males and females [6]. The knees were modeled with population average ligament stiffness [26, 37], which may differ from those seen in osteoarthritic knees. Clinical intuition suggests that ligament stiffness may

2017 Knee Society Proceedings

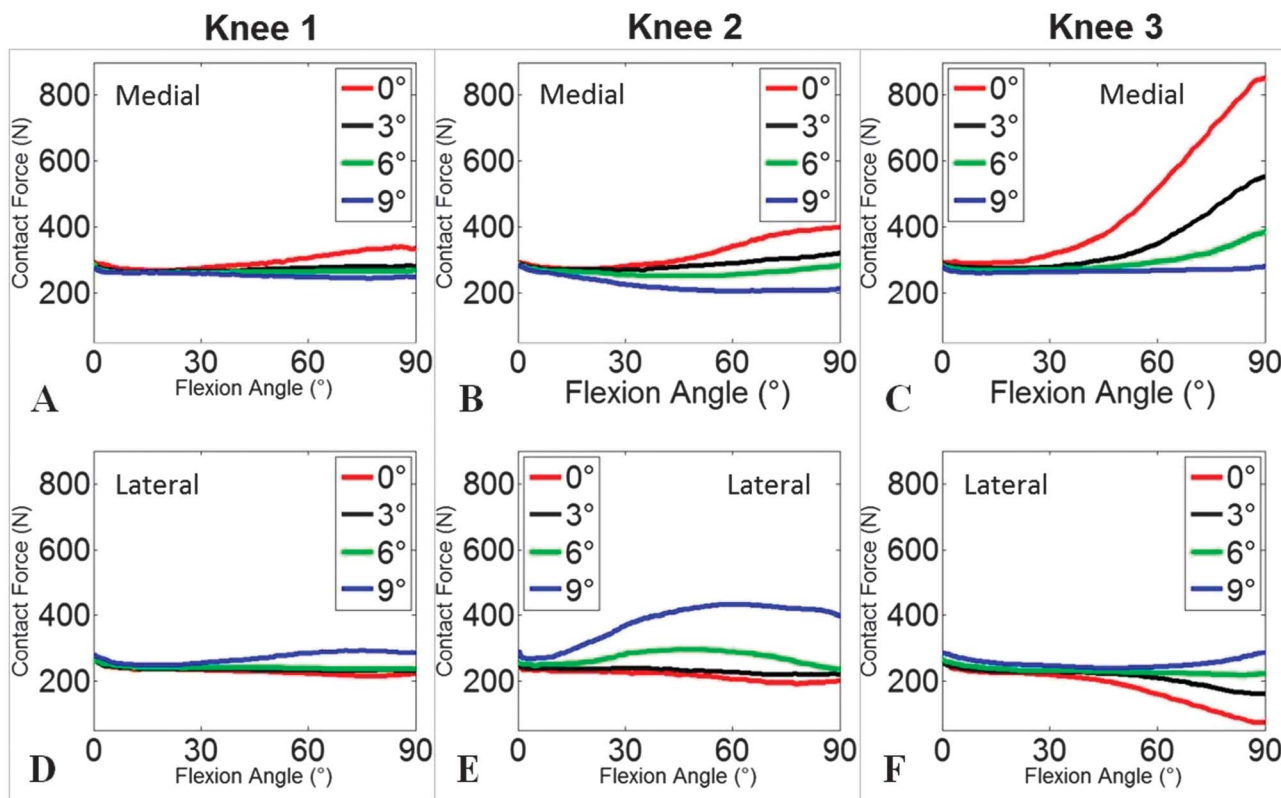


Fig. 5 A-F Articular contact forces in the medial and lateral compartments predicted by the three knee models during a flexion path from 0° to 90° were altered when the femoral component had been rotated externally at implantation by 0°, 3°, 6°, and 9° relative to the posterior condylar axis: (A-C) medial contact force; (D-F) lateral contact force.

increase with osteoarthritis. If so, our ligament force predictions represent a lower bound of those that might occur. Furthermore, increasing or decreasing the ligament stiffness across the three knee models would cause a proportionate change in the ligament forces. However, this would not change our finding that geometric factors are important drivers of variations in ligament force from knee to knee. Moreover, ligament balancing techniques differ among surgeons and their effects on ligament properties are unknown. Therefore, we capitalized on the model’s ability to standardize ligament slack length and stiffness across all knees to control these variables and better isolate the impact of geometric

variations on knee biomechanics. Subject-specific properties could be included in future work by directly testing cadaveric tissue and including them in the model or by calibrating ligament stiffness to tests of varus and valgus laxity. Another limitation was that we used models of only three knees that were nonarthritic and neutrally aligned; however, this sample was adequate to underscore our main finding that femoral component external rotation effects vary from knee to knee based on geometries of the bones and ligament insertions as well as the implant size and placement. Moreover, our study represents advancement over previous models using a single knee [7, 9]. Finally, our model did not

include the effect of implant subsidence and viscoelastic effects were minimized, because the models were flexed slowly (1°/sec). Thus, the model represents the time-zero biomechanical response of the knee.

This study has further limitations; muscle tensions are not included in this simulation because the loads used in our study represent those applied during intraoperative examination in which the knee is passively flexed by the surgeon [20]. The effect of femoral component external rotation may be accentuated under functional loading scenarios such as gait or stair descent. Nevertheless, differences in kinematics, ligament tension, and contact force were apparent even in response to the

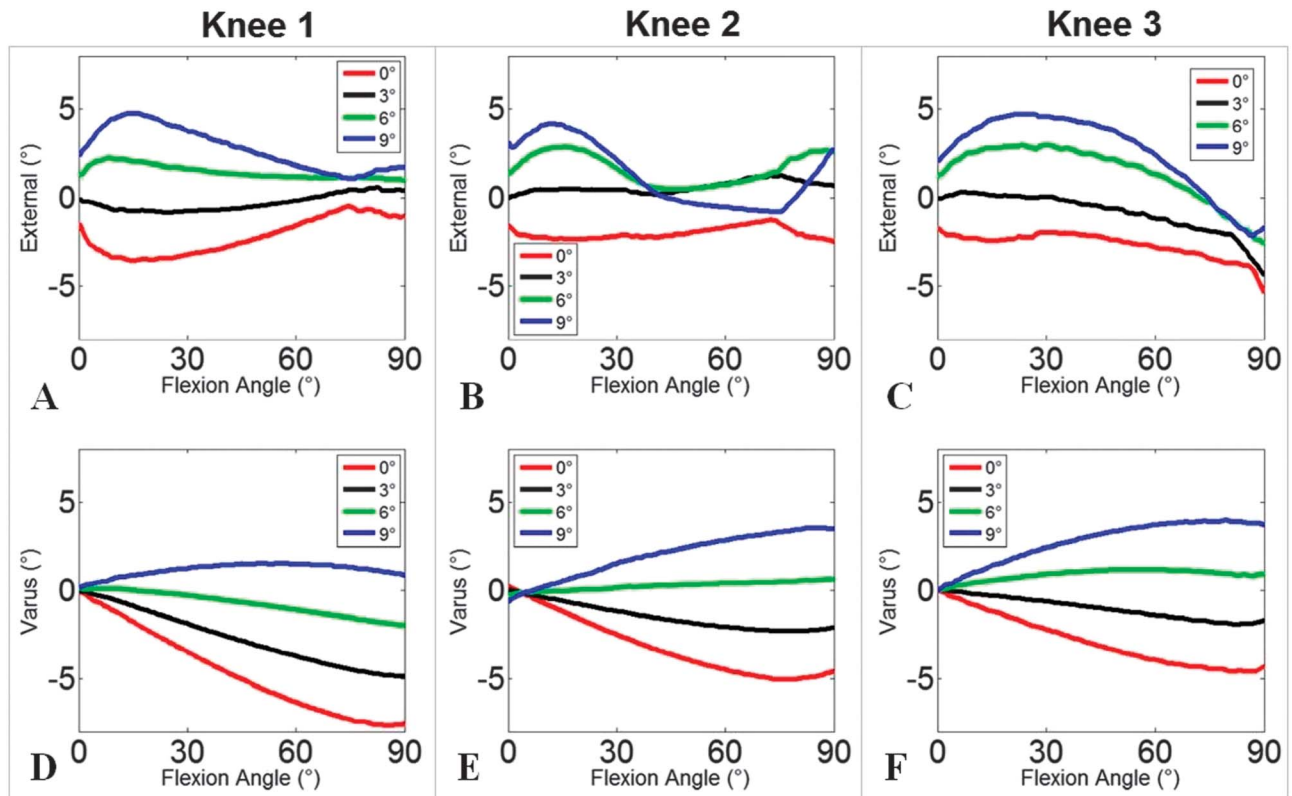


Fig. 6 A-F Tibiofemoral kinematics were predicted by the three knee models during flexion from 0° to 90° when the femoral component had been rotated externally by 0°, 3°, 6°, and 9° relative to the posterior condylar axis: (A-C) internal-external rotation where increasing magnitude indicates external rotation of the tibia; (D-F) varus-valgus rotation where increasing magnitude indicates varus angulation of the tibia.

relatively small amount of compression applied in this study, which simulates intraoperative assessment. Moreover, the femoral component was rotated about the femoral intramedullary axis to simulate the technique used for this prosthesis design; other locations of the axis of rotation could easily be studied using the model. Although rotation of the femoral component impacts patellofemoral joint function, we focused this work on the impact of this variable on tibiofemoral joint biomechanics because this is also an important area of study [30]; patellofemoral joint biomechanics will be the focus of future work.

Our first finding was that femoral component external rotation unloaded the MCL between 30° and 90° of flexion. However, the predicted MCL tension and the amount of offloading with external rotation were not consistent from knee to knee (Fig. 4A-C). This variability may be explained by differences in resection of posteromedial bone, which ranged from 12 mm in knee one to 7 mm in knee two compared with an implant thickness of 8 mm (Fig. 1). Greater resection of posteromedial bone more greatly decreases the flexion gap on the medial side and therefore more drastically offloads the MCL. In contrast, LCL tension was less influenced by femoral

component external rotation, likely because the LCL is approximately two times less stiff and is less isometric than the MCL in flexion [26, 34, 37], making it less sensitive to changes in femoral component external rotation.

Our second finding was that the decrease in MCL force with femoral component external rotation coincided with alterations in contact force. The decrease in medial compartment contact force agrees with findings from a previous model of a single knee [6]. Paralleling our findings with MCL force, the predicted decrease in medial compartment contact force was inconsistent from knee to knee through the range of flexion. Moreover, the

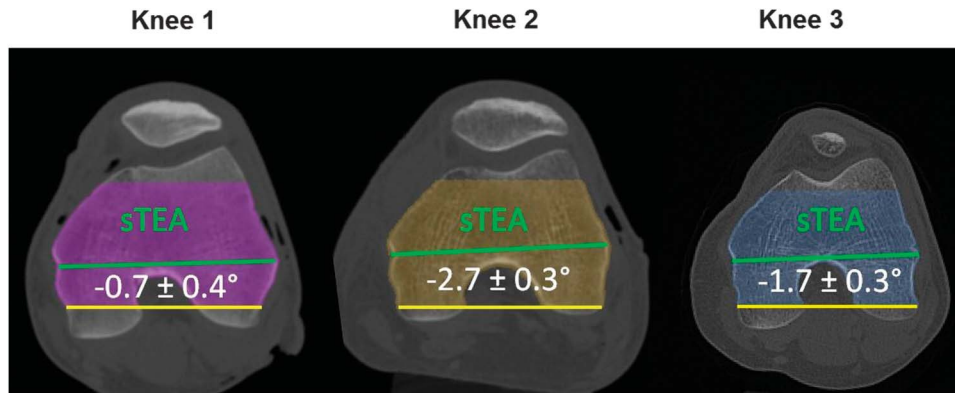


Fig. 7 Angle between the sTEA (green line) and the posterior femoral condylar cut (yellow line) on an axial cross-section of the femur viewed distally to proximally. Measurements were performed five times and the mean value and SD are reported. These images show the relative angulation of the two axes with the cuts oriented in 3° external rotation relative to the posterior condylar axis. A negative sign indicates external rotation of the posterior condylar cuts relative to the sTEA.

variations in the difference in contact forces between the medial and lateral compartments are clinically relevant because they exceeded magnitudes (67 N) that have been reported to coincide with reduced patient-reported outcomes at early postoperative time points [11]. Interestingly, model predictions of contact forces in the medial and lateral compartments corroborated corresponding intraoperative measurements with the medial compartment carrying approximately 100 N more

force than the lateral compartment at 3° external rotation of the femoral component [20].

With regard to tibiofemoral kinematics, external tibial rotation from full extension to 20° of flexion with the femoral component externally rotated contrasts with the typical screw home mechanism where the tibia rotates internally over the first 20° of flexion [5, 10, 14, 36]. This behavior is likely related to the offset of the tibia in external rotation at full extension, which makes

the contact forces drive the knee into external rotation (Fig. 5A-F). The sudden change in the direction of tibial axial rotation between 70° and 80° of flexion in the three knees was likely caused by cam-post contact in this PS design. Our kinematic findings of abnormal screw home motion and varus angulation with flexion agree with a previous cadaveric experiment of the femoral component in a cruciate-retaining (CR) design [21]. However, the effect of external rotation on

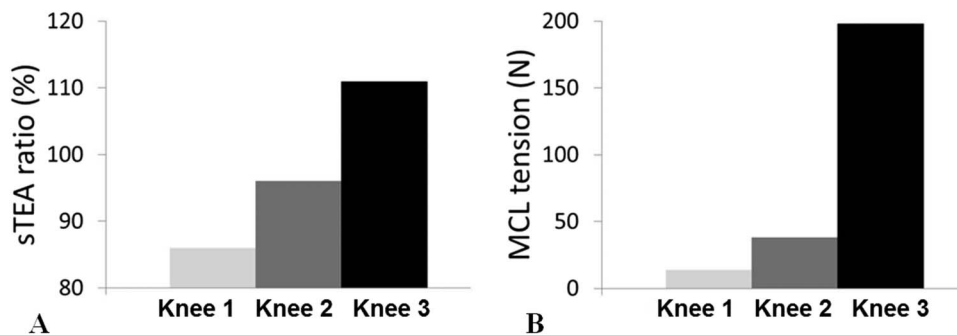


Fig. 8 A-B (A) Ratio between the posterior and distal distances of the medial aspect of the sTEA and the respective posterior and distal condylar cuts. (B) Force carried by the MCL in each knee at 90° flexion with femoral component rotation of 3° relative to the posterior condylar axis.

2017 Knee Society Proceedings

posterior cruciate ligament (PCL) function in CR designs was not the focus of this study.

Not surprisingly, 3° of external rotation of the femoral component with respect to the posterior condylar axis did not consistently align with the sTEA of each knee in this group of nonarthritic, neutrally aligned tibiofemoral geometries, which corroborates previous reports [29]. This inconsistent alignment, along with femoral component sizing dictated by the anterior referencing approach, contributed to variations in the amount of bone resected from the medial and lateral posterior condyles (Fig. 7). We found that, as a result, the predicted maximum MCL force at 3° of external rotation of the femoral component differed from knee to knee reaching 198 N in knee three (Fig. 4C). This magnitude of maximum MCL force likely is clinically relevant because it is approximately 37% of the mean failure load of the MCL (534 N) and may cause subfailure damage and stretching of this ligament [23, 24, 26]. Because we controlled for the stiffness and slack of the ligaments and used the same implant design across knees, other variables must explain the knee-to-knee variations in MCL force. They include the sizes of the bones and implants, the locations of the ligament insertions, and component positioning through anterior referencing. We began to incorporate these variables into a single measure: the ratio of the distances of the medial epicondylar sulcus (that is, the medial aspect of the sTEA) to the posterior and distal cuts of the medial femoral condyle (Fig. 3). Interestingly, as this ratio increased, so did the force carried by the MCL (Fig. 8A-B). We also observed that the MCL consistently started to carry force at approximately 30° flexion (Fig. 4) where the femoral component

transitions from the distal radius in extension to the posterior radius in flexion. Thus, if the distances from the femoral insertion of the MCL to the posterior and the distal cuts of the implant were the same (ratio of 1), more constant tension of the MCL could be achieved from 0° to 90° of knee flexion.

In conclusion, our modeling approach allows for a holistic assessment of knee function enabling the prediction of kinematics and contact and ligament forces through a range of flexion. Using the model to standardize ligament properties and limb alignment from knee to knee, we found that subtle geometric variations including the ratio of distances from the femoral insertion of the MCL to the posterior and distal cuts were related to clinically relevant variations in MCL tension and medial contact force between knees. Accordingly, we found with larger ratios that (1) the difference in compartmental contact forces could exceed levels that have been reported to coincide with reduced patient-reported outcomes [11, 12]; and (2) MCL tension could exceed levels that may cause subfailure damage and stretching in this ligament through flexion [23, 24]. Gaps in knowledge that can also be addressed using a computational modeling framework include characterizing the isolated influence of and interactions between other important variables such as ligament properties, implant design including those that retain the PCL, and implant placement. Finally, the influence of the commonly used posterior referencing technique on knee biomechanics can also be addressed. Altogether, based on our initial findings, we speculate that it may be important to identify the posterior and distal locations of the femoral component in PS TKA with respect to the proximal insertions of the

collateral ligaments such that a ratio of 1 is achieved to obtain more consistent ligament loads through flexion.

Acknowledgments We thank Joe Lipman MS, for his valuable contributions to defining the methods for virtually installing the implant components.

References

1. Anouchi YS, Whiteside LA, Kaiser AD, Milliano MT. The effects of axial rotational alignment of the femoral component on knee stability and patellar tracking in total knee arthroplasty demonstrated on autopsy specimens. *Clin Orthop Relat Res.* 1993;287:170-177.
2. Barrack RL, Schrader T, Bertot AJ, Wolfe MW, Myers L. Component rotation and anterior knee pain after total knee arthroplasty. *Clin Orthop Relat Res.* 2001;392:46-55.
3. Berger RA, Crossett LS, Jacobs JJ, Rubash HE. Malrotation causing patellofemoral complications after total knee arthroplasty. *Clin Orthop Relat Res.* 1998;356:144-153.
4. Berger RA, Rubash HE, Seel MJ, Thompson WH, Crossett LS. Determining the rotational alignment of the femoral component in total knee arthroplasty using the epicondylar axis. *Clin Orthop Relat Res.* 1993;286:40-47.
5. Cassidy KA, Tucker SM, Rajak Y, Kia M, Imhauser CW, Westrich GH, Heyse TJ. Kinematics of passive flexion following balanced and overstuffed fixed bearing unicompartmental knee arthroplasty. *Knee.* 2015;22:542-546.
6. Castelli CC, Falvo DA, Iapicca ML, Gotti V. Rotational alignment of the femoral component in total knee arthroplasty. *Ann Transl Med.* 2016;4:4.
7. Chen Z, Wang L, Liu Y, He J, Lian Q, Li D, Jin Z. Effect of component malrotation on knee loading in total knee arthroplasty using multi-body dynamics modeling under a simulated walking gait. *J Orthop Res.* 2015;33:1287-1296.
8. Claes S, Vereecke E, Maes M, Victor J, Verdonk P, Bellemans J. Anatomy of the anterolateral ligament of the knee. *J Anat.* 2013;223:321-328.
9. Clary CW, Fitzpatrick CK, Maletsky LP, Rullkoetter PJ. The influence of total knee arthroplasty geometry on mid-flexion stability: an experimental and

2017 Knee Society Proceedings

- finite element study. *J Biomech.* 2013;46:1351-1357.
10. Fiacchi F, Zambianchi F, Digennaro V, Ricchiuto I, Mugnai R, Catani F. In vivo kinematics of medial unicompartmental osteoarthritic knees during activities of daily living. *Knee.* 2014;21(Suppl 1):S10-14.
 11. Gustke KA, Golladay GJ, Roche MW, Elson LC, Anderson CR. A new method for defining balance: promising short-term clinical outcomes of sensor-guided TKA. *J Arthroplasty.* 2014;29:955-960.
 12. Gustke KA, Golladay GJ, Roche MW, Jerry GJ, Elson LC, Anderson CR. Increased satisfaction after total knee replacement using sensor-guided technology. *Bone Joint J.* 2014;96:1333-1338.
 13. Kennedy MI, Claes S, Fuso FA, Williams BT, Goldsmith MT, Turnbull TL, Wijdicks CA, LaPrade RF. The anterolateral ligament: an anatomic, radiographic, and biomechanical analysis. *Am J Sports Med.* 2015;43:1606-1615.
 14. Kia M, Schafer K, Lipman J, Cross M, Mayman D, Pearle A, Wickiewicz T, Imhauser C. A multibody knee model corroborates subject-specific experimental measurements of low ligament forces and kinematic coupling during passive flexion. *J Biomech Eng.* 2016;138:051010.
 15. Kim YH, Park JW, Kim JS, Park SD. The relationship between the survival of total knee arthroplasty and postoperative coronal, sagittal and rotational alignment of knee prosthesis. *Int Orthop.* 2014;38:379-385.
 16. Kim YH, Sohn KS, Kim JS. Range of motion of standard and high-flexion posterior stabilized total knee prostheses. A prospective, randomized study. *J Bone Joint Surg Am.* 2005;87:1470-1475.
 17. LaPrade RF, Engebretsen AH, Ly TV, Johansen S, Wentorf FA, Engebretsen L. The anatomy of the medial part of the knee. *J Bone Joint Surg Am.* 2007;89:2000-2010.
 18. LaPrade RF, Morgan PM, Wentorf FA, Johansen S, Engebretsen L. The anatomy of the posterior aspect of the knee. An anatomic study. *J Bone Joint Surg Am.* 2007;89:758-764.
 19. Lutzner J, Krummenauer F, Gunther KP, Kirschner S. Rotational alignment of the tibial component in total knee arthroplasty is better at the medial third of tibial tuberosity than at the medial border. *BMC Musculoskelet Disord.* 2010;11:57.
 20. Meneghini RM, Ziemba-Davis MM, Lovro LR, Ireland PH, Damer BM. Can intraoperative sensors determine the 'target' ligament balance? early outcomes in total knee arthroplasty. *J Arthroplasty.* 2016;31:2181-2187.
 21. Miller MC, Berger RA, Petrella AJ, Karmas A, Rubash HE. Optimizing femoral component rotation in total knee arthroplasty. *Clin Orthop Relat Res.* 2001;392:38-45.
 22. Murakami AM, Hash TW, Hepinstall MS, Lyman S, Nestor BJ, Potter HG. MRI evaluation of rotational alignment and synovitis in patients with pain after total knee replacement. *J Bone Joint Surg Br.* 2012;94:1209-1215.
 23. Panjabi MM, Huang RC, Cholewicki J. Equivalence of single and incremental subfailure stretches of rabbit anterior cruciate ligament. *J Orthop Res.* 2000;18:841-848.
 24. Panjabi MM, Yoldas E, Oxland TR, Crisco JJ 3rd. Subfailure injury of the rabbit anterior cruciate ligament. *J Orthop Res.* 1996;14:216-222.
 25. Poilvache PL, Insall JN, Scuderi GR, Font-Rodriguez DE. Rotational landmarks and sizing of the distal femur in total knee arthroplasty. *Clin Orthop Relat Res.* 1996;331:35-46.
 26. Robinson JR, Bull AM, Amis AA. Structural properties of the medial collateral ligament complex of the human knee. *J Biomech.* 2005;38:1067-1074.
 27. Saigo T, Tajima G, Kikuchi S, Yan J, Maruyama M, Sugawara A, Doita M. Morphology of the insertions of the superficial medial collateral ligament and posterior oblique ligament using 3-dimensional computed tomography: a cadaveric study. *Arthroscopy.* 2017;33:400-407.
 28. Sanchez AR 2nd, Sugalski MT, LaPrade RF. Anatomy and biomechanics of the lateral side of the knee. *Sports Med Arthrosc.* 2006;14:2-11.
 29. Schnurr C, Nessler J, Konig DP. Is referencing the posterior condyles sufficient to achieve a rectangular flexion gap in total knee arthroplasty? *Int Orthop.* 2009;33:1561-1565.
 30. Scuderi GR, Komistek RD, Dennis DA, Insall JN. The impact of femoral component rotational alignment on condylar lift-off. *Clin Orthop Relat Res.* 2003;410:148-154.
 31. Sun T, Lu H, Hong N, Wu J, Feng C. Bony landmarks and rotational alignment in total knee arthroplasty for Chinese osteoarthritic knees with varus or valgus deformities. *J Arthroplasty.* 2009;24:427-431.
 32. Thienpont E, Schwab PE, Paternostre F, Koch P. Rotational alignment of the distal femur: anthropometric measurements with CT-based patient-specific instruments planning show high variability of the posterior condylar angle. *Knee Surg Sports Traumatol Arthrosc.* 2014;22:2995-3002.
 33. Victor J. Rotational alignment of the distal femur: a literature review. *Orthop Traumatol Surg Res.* 2009;95:365-372.
 34. Victor J, Wong P, Witvrouw E, Sloten JV, Bellemans J. How isometric are the medial patellofemoral, superficial medial collateral, and lateral collateral ligaments of the knee? *Am J Sports Med.* 2009;37:2028-2036.
 35. Whiteside LA. Choosing your implant: cementless, patella sparing, and posterior cruciate ligament retaining. *J Arthroplasty.* 2005;20:10-11.
 36. Wilson DR, Feikes JD, Zavatsky AB, O'Connor JJ. The components of passive knee movement are coupled to flexion angle. *J Biomech.* 2000;33:465-473.
 37. Wilson WT, Deakin AH, Payne AP, Picard F, Wearing SC. Comparative analysis of the structural properties of the collateral ligaments of the human knee. *J Orthop Sports Phys Ther.* 2012;42:345-351.